II. STRUCTURE AND PROPERTIES DURING AGING OF AN Al-Cu-Li-Ag-Mg ALLOY, WELDALITE™049

Frank W. Gayle, Frank H. Heubaum, and Joseph R. Pickens

1. INTRODUCTION

An Al-Cu-Li-Ag-Mg alloy Weldalite™ 049 was recently introduced as an ultra-high strength alloy (700 MPa yield strength in artificially aged tempers) with good weldability (1). In addition, the alloy exhibits an extraordinary natural aging response (440 MPa yield strength (YS) in the unstretched condition) and a high ductility reversion condition which may be useful as a cold-forming temper (1,2). In contrast to other Al-Li alloys, these properties can essentially be obtained with or without a stretch or other coldworking operation prior to aging.

Preliminary studies have revealed that the T4 temper (no stretch, natural age) is strengthened by a combination of GP zones and δ' (Al_3Li) (2). The T6 temper (no stretch, aged at 180°C to peak strength) was reported to be strengthened primarily by the T_1 phase (Al_2CuLi) with a minor presence of a θ'-like (Al_2Cu) phase (3). On the other hand, a similar but lower solute-containing alloy was reported to contain Ω, (stoichiometry unknown), θ', and S' in the peak strength condition (4). The purpose of the present study is to further elucidate the strengthening phases in Weldalite™ 049 in the unstretched tempers, and to follow the development of the microstructure from the T4 temper through reversion (180°C for 5-45 minutes) to the T6 temper.

2. EXPERIMENTAL PROCEDURE

The alloy was examined in two product forms, sheet and extruded bar, with the compositions given in Table 1. The alloys were heat treated as follows: solutionized at 503°C for 1 hour, quenched in cold water, and allowed to naturally age at room temperature to the T4 condition. (The T4 temper was defined as >1000 hours at ambient temperature and was used as the starting condition for all artificially aged tempers.) Artificial aging was carried out by heating specimens in a circulating air furnace at 180°C. The sheet specimens were used for the T4 and reversion studies, whereas extrusions were examined in other aged conditions.

Specimens for transmission electron microscopy (TEM) analysis were twin-jet electropolished at -20°C and 12 volts in a solution of 30% HNO_3 in methanol. After polishing, the specimens were dipped in a solution of 50% HNO_3 in H_2O to remove superficial Ag which had re-deposited from the electrolyte during polishing.

TABLE 1

Alloy Compositions (wt.%)

Form	Cu	Li	Mg	Ag	Zr	Si	Fe
Sheet	6.0	1.3	0.4	0.4	0.18	0.04	0.05
Extruded bar	4.50	1.16	0.36	0.37	0.13	0.01	0.03

3. RESULTS

The aging response was monitored using Rockwell B hardness measurements. Natural aging resulted in a very high T4 hardness, R_B 80, corresponding to a tensile strength of about 585 MPa. A short artificial aging period, e.g., 5-45 minutes at 180°C, then led to a reversion with associated loss of hardness (see Figure 1). Further aging at 180°C for 16-24 hours resulted in peak hardness. Also shown in Figure 1 (dashed curve) is the *room temperature* aging response after a reversion treatment (45 minutes at 180°C. It is clear that after reversion the alloy re-ages at room temperature back to the T4 hardness level, albeit only after an extended incubation period. Typical tensile properties for various conditions are extremely high, as shown in Table 2.

TABLE 2

Longitudinal Tensile Properties
(25 mm gauge; $\dot{\varepsilon} = 3 \times 10^{-4}\ s^{-1}$)

Temper	Aging Practice	YS MPa	UTS MPa	El. %
T4	RT/1000 h	438	585	15.5
Reversion	180°C/15 min	280	480	25.5
Revert/re-age	180°C + RT/10^4h	440	610	11.0
T6	180°C/24 h	680	720	4.0

RT = room temperature

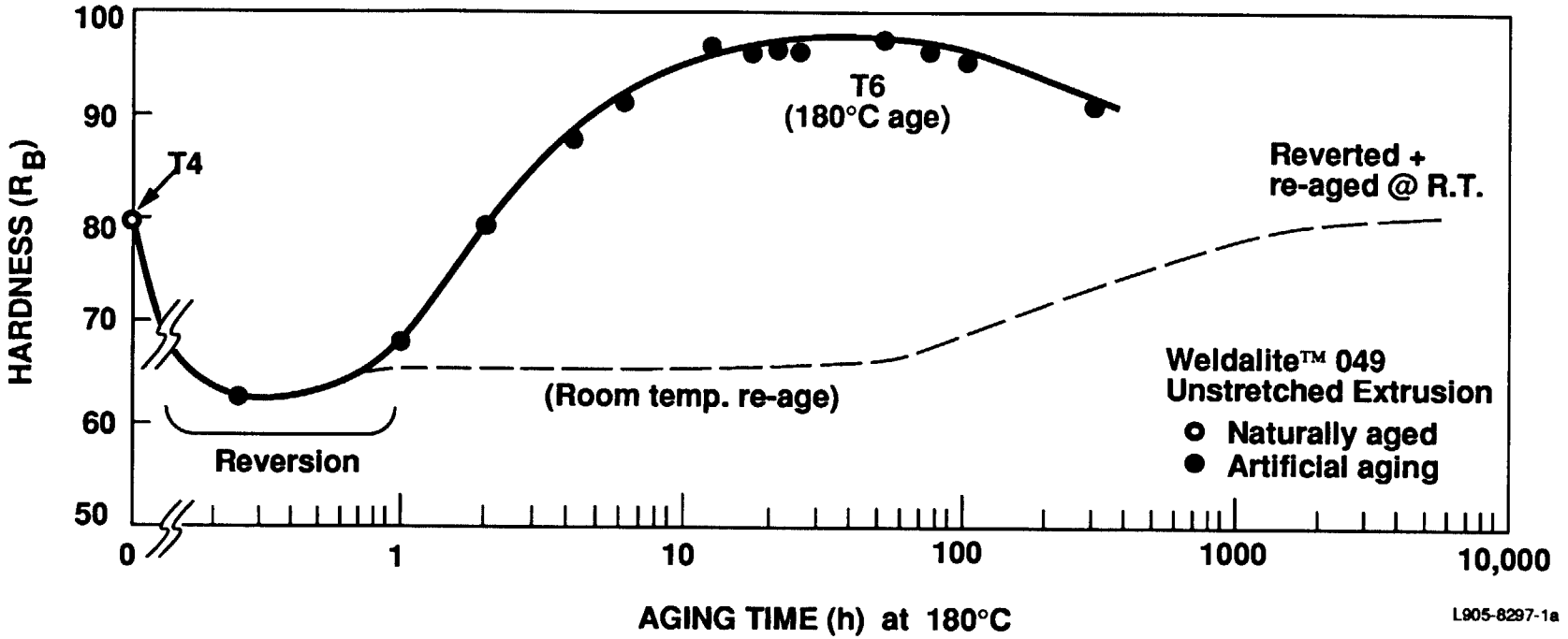

Figure 1 Aging curve at 180°C (Rockwell B hardness) from T4 to overaged condition. Also shown (dashed) is the natural aging response of the alloy following a reversion treatment of 180°C/45 minutes, showing that after an extended incubation period, re-aging at room temperature results in a return of T4 hardness.

The T4 structure exhibited a remarkably well-developed GP zone structure (Fig.2a) compared with other aluminum alloys aged at room temperature. Continuity of <100> streaks in the diffraction patterns indicates that these are classical GPI zones consisting of monolayers of Cu lying in disks on {100} matrix planes (5). δ' was also present, both as 1-2 nm spheres in a very fine uniform distribution, and as characteristic envelopes surrounding the Zr-rich α' similar to that seen in Zr-bearing higher-lithium alloys (6,7).

The reversion treatment was found to dissolve δ' and coarsen the GP zone structure. Re-aging at room temperature reprecipitated δ' and additional very fine GP zones (Fig. 3), resulting in a complex microstructure. The GP zones, all lying on {100} planes, exist in three distributions with two major populations:

1) homogeneously nucleated zones, 12-15 nm } remaining after
2) zones nucleated on α', 12-15 nm } reversion
3) homogeneously nucleated zones, 2.5-5 nm, precipitated during re-aging.

The δ' phase, although present as a small volume fraction, also assumed at least three distributions:

1) uniformly distributed, 1-2 nm spheres
2) heterogeneously nucleated envelopes on α'
3) coating the faces of larger GPI zones.

Artificial aging beyond 45 minutes brought the alloy out of the reversion well. After aging at 180°C for two hours (Figure 4), the structure contained a wealth of precipitate phases: GPI zones (minor volume fraction), θ' (Al_2Cu plates lying on {100}), T_1 (Al_2CuLi plates lying on {111}), and S' (Al_2CuMg laths on {210} extended in <001> directions). Continued aging to peak strength and beyond (16-48 hours) dissolved the GP zones leaving θ', T_1, and S' in substantial numbers, with T_1 appearing as the largest volume fraction. In the T6 condition, the precipitates remain quite thin and in a good dispersion, with T_1 typically one unit cell in thickness, and θ' and S' less than 2-3 nm in thickness.

An additional unidentified precipitate was observed (Fig. 5) for aging times from 2 to 48 hours. This precipitate lies on $\{110\}_{matrix}$

Figure 2 T4 structure, showing advanced GP zone structure (TEM BF). Continuous streaks in the SADP indicate the zones are GPI zones.

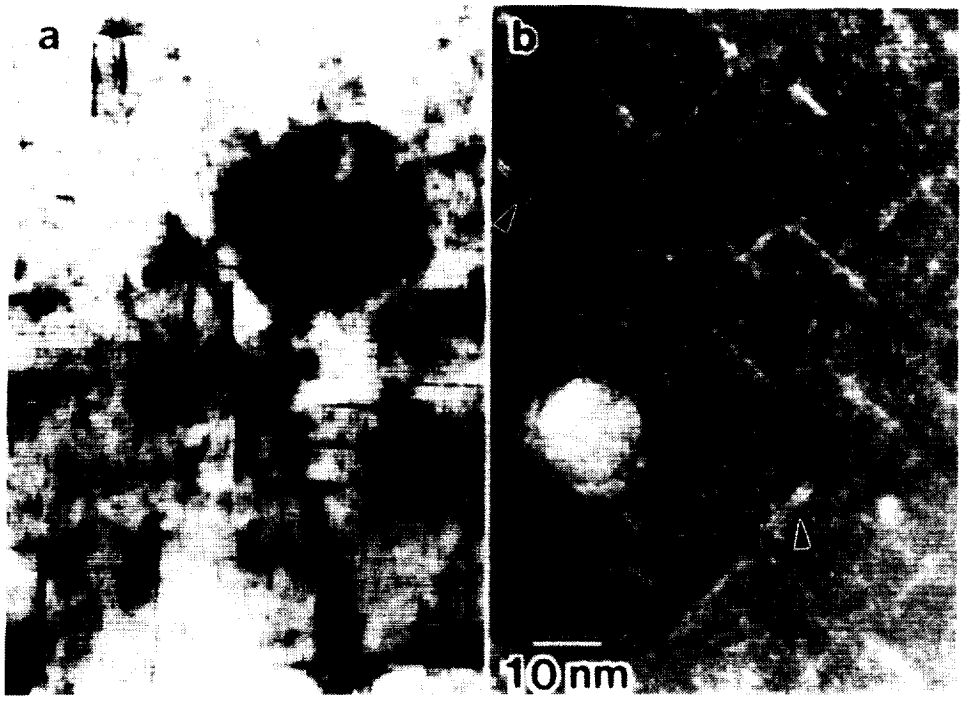

Figure 3 Microstructure after reversion (180°C/45 min) and re-aging at room temperature for 6400 hours. a) Bright field image showing very fine, duplex GP zone structure. b) Superlattice dark field image showing various distributions of δ', including the precipitation of δ' on the faces of larger GP zones (arrows). Large $L1_2$-ordered α' dispersoid is also imaged brightly.

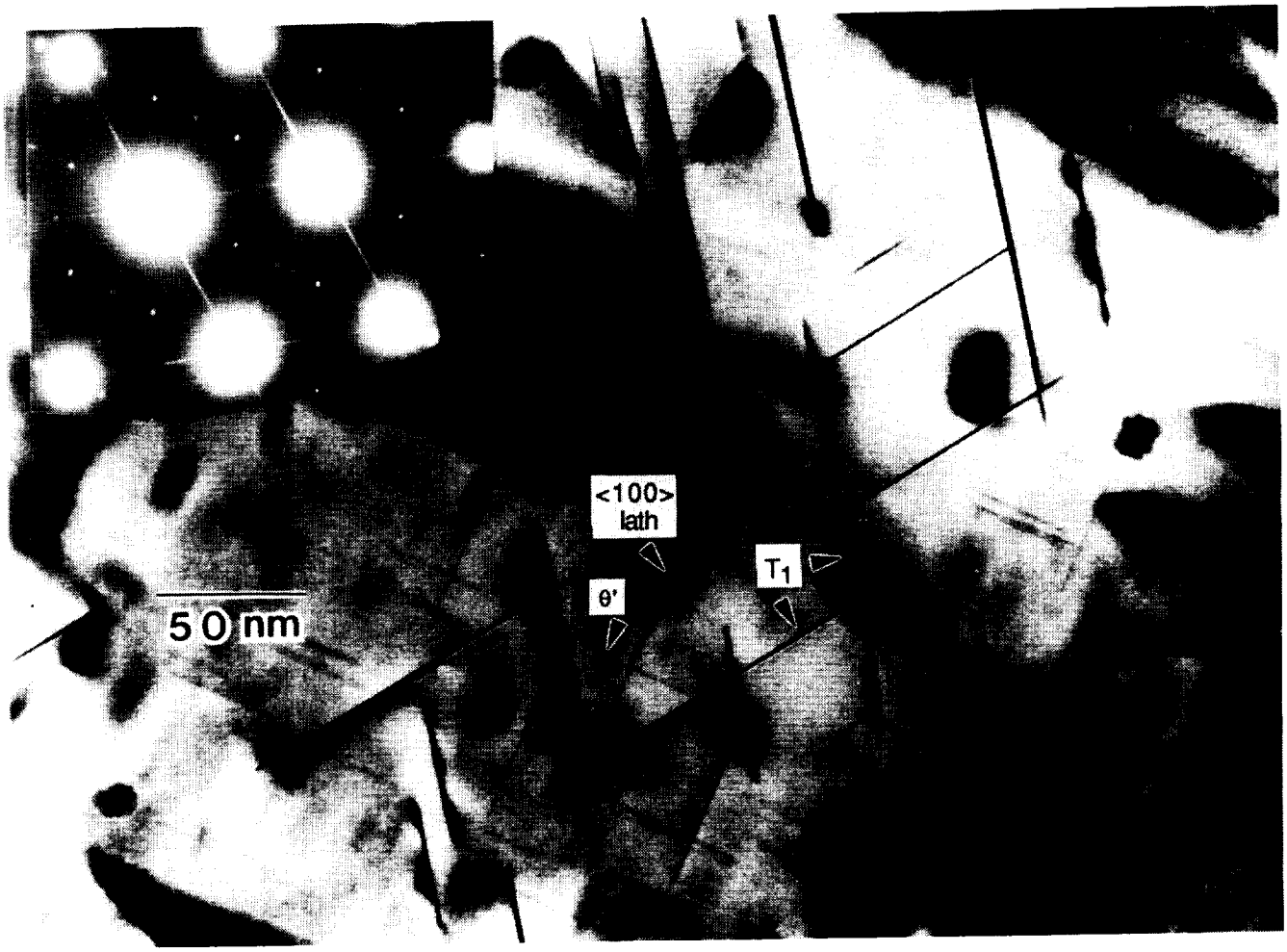

Figure 4 Aged 180°C/2 hours, showing T_1 lying on {111}, θ' lying on {100}, and laths extending in the [100] direction (Beam direction B=[011]).

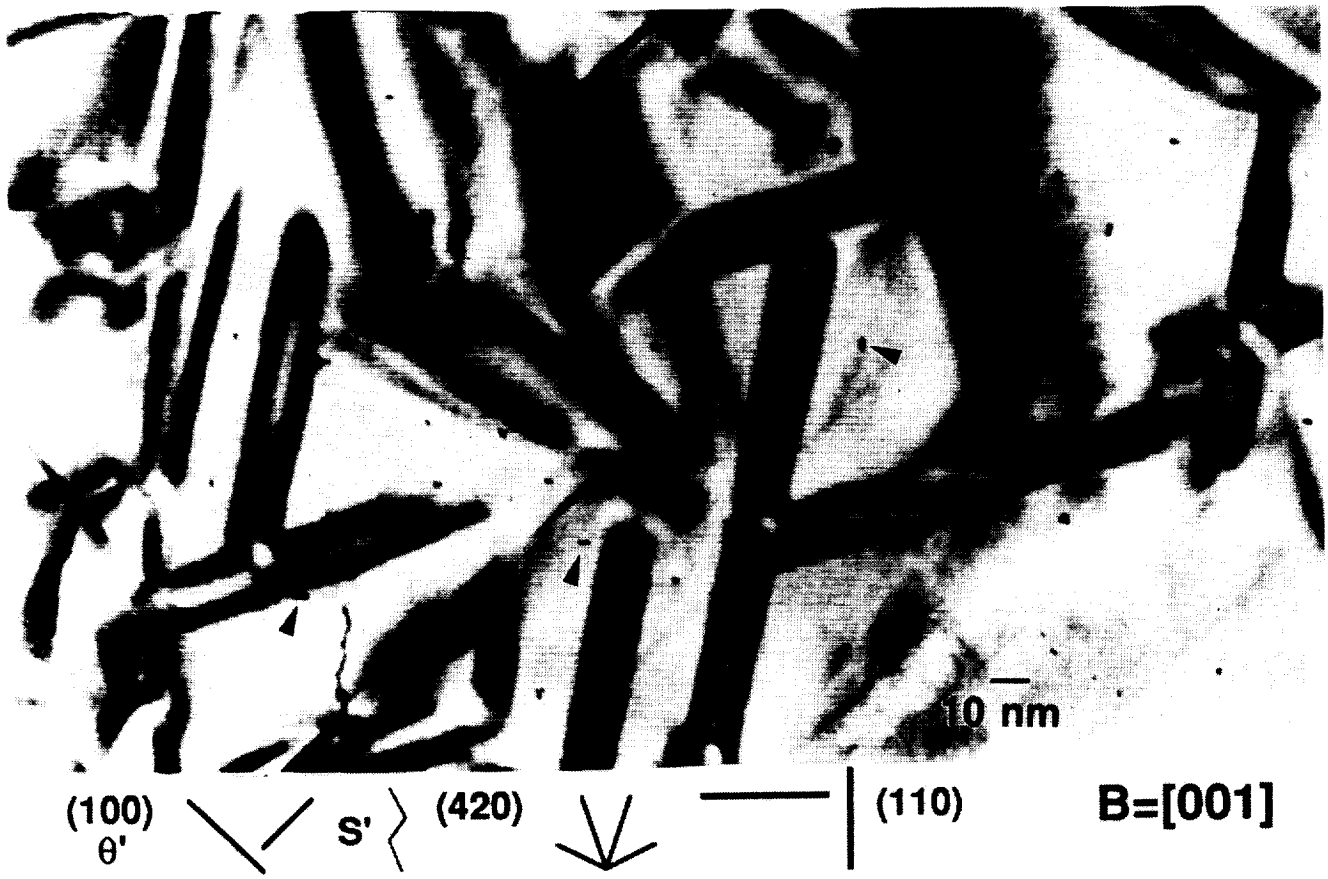

Figure 5 Aged 180°C/2 hours, showing S', lying on {210} planes, and another lath-like phase (arrows) lying on {110} planes (θ' plates on [100] planes are also visible. Wide, dark bands are T_1 plates viewed at an oblique angle.) (B=[001]).

planes, appearing as laths extending in <001> $_{matrix}$ directions. The precipitate remained very small for all aging times from 2 to 48 hours, with cross sections of 1.5 x 4.5 nm when observed end on.

A summary of the precipitate distribution as a function of aging condition is given in Figure 6. For heuristic purposes, the proposed new phase described above is designated by the Greek letter ν.

4. DISCUSSION

Weldalite™ 049 shows extraordinary T4 hardness and strength, comparable to many aerospace alloys artificially aged to peak strength. The strength is derived from a very well developed GP zone structure and the precipitation of δ'. Accelerated zone formation has been reported in Al-6Cu-0.3Mn alloys with 0.02-0.12 Mg (8) and 0.18 Mg (9) additions, and was attributed to enhanced nucleation at Mg-vacancy complexes, as previously proposed by Kelly and Nicholson (5). It is likely that Mg produces a similar effect in Weldalite™ 049. That is, the Mg atoms enhance the equilibrium vacancy concentration during solution heat treatment and help retain the vacancies through the quenching operation. These vacancies may provide a dual beneficial effect on T4 properties -- enhanced nucleation and also increased diffusivity. Whether this natural aging process is enhanced by the presence of Ag is being addressed in another study.

Room temperature precipitation of GP zones and δ' after the reversion treatment is in part made possible by the reduction in solubility of Cu and Li upon cooling from 180°C to room temperature. The long delay before a significant increase in strength upon subsequent natural aging is unexpected at first glance, considering the rapid aging response following solution heat treatment. However, the annealing out of quenched-in excess vacancies during the original aging and reversion treatments, and solute depletion associated with the coarser GP zones present after reversion likely contribute to the long incubation period.

It should be noted that all GP zones observed in this alloy are believed to be GPI zones based on the continuous nature of <100> streaks in the diffraction patterns. In the classical view (5), GPI zones are monolayers of nearly pure Cu lying in disks on {100} matrix planes. To our knowledge, this alloy system is the first one in which GPI zone nucleation on the Zr-rich α' dispersoid is reported. The unusual post-

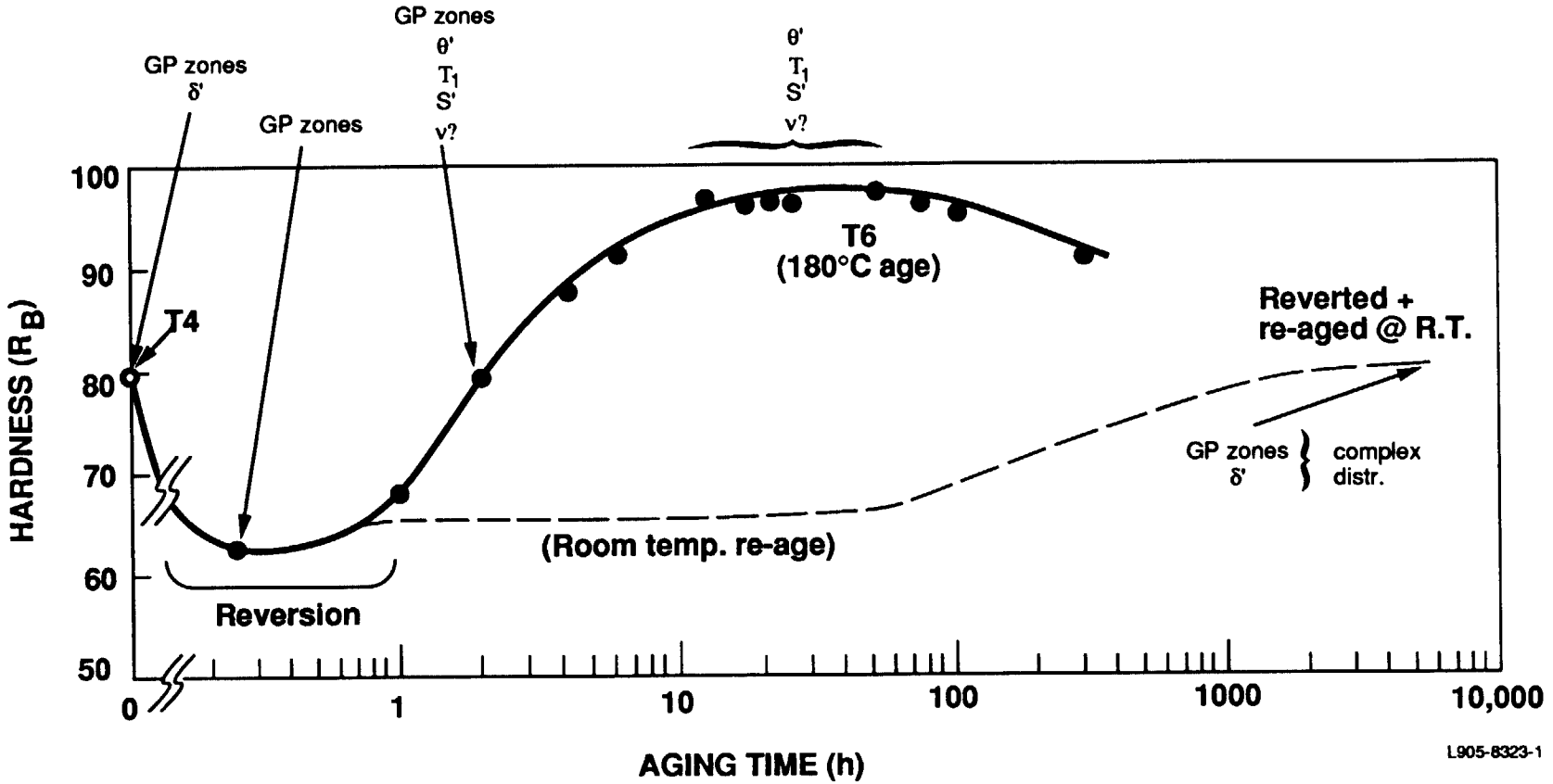

Figure 6 Summary of aging sequence: Aging curve and associated strengthening precipitates.

reversion precipitation of δ' on the faces of the larger GP zones during room temperature aging is not unique; in addition to the Weldalite™ alloy system (2), DeJesus and Ardell (11) have recently seen similar behavior in the higher Li-containing alloy 2090 (Al-2.7Cu-2.3Li-0.12Zr) after natural aging. These observations are but two new additions to the many examples (2) of heterogeneous nucleation of coherent phases in Al-Li-(Cu,Mg,Zr) systems.

The 2 hour aging treatment yields a transition state in which GP zones are still present along with the various strengthening phases that are present in the T6 temper. Longer artificial aging times produce the T6 structure, which is strengthened by a combination of several phases, including θ', S', and T_1. The T6 condition may indeed represent a metastable six-phase equilibrium between the aluminum alloy matrix, several strengthening precipitates (θ', T_1, S' and ν), and the dispersoid α'. (Six phases in stable or metastable equilibrium over a range of temperature is the maximum allowed by Gibbs' phase rule in a six component system.) T_1 is likely the dominant strengthening phase, based on apparent number density, morphology and distribution.

In Al-Cu-Mg alloys S' is reported to assume two different habits. In the first, the precipitates occur as laths lying on {210} planes, extending in <001> directions (11, 12). Corrugated precipitate sheets approximating a {110} plane may form from two or more variants lying on {210} planes with a common <100> direction. The other habit is rodlike, extending in {100} directions, with some tendency to cluster on {110} planes (13).

The proposed ν phase has characteristics similar to S'. Both phases are lath-like with the longest dimension extending in the $<100>_{matrix}$ direction. However, a clear distinction between the two phases exists, as shown in Figure 5. The laths visible in this B=[100] micrograph are all viewed end-on, with the length projected into the plane of the photomicrograph. The S' is visible both as individual laths lying on {210} planes, and as the occasional corrugated sheet which is composed of two {210} variants. This corrugated sheet approximates a {110} habit plane. Also seen are laths which lie on {110} planes. These laths are 1.5 nm in thickness by 4.5 nm in width, and appear as individual laths with a {110} habit rather than corrugated composites of S'. Therefore, these individual laths with a {110} habit are either a new phase, or else S' with a new habit and/or a new orientation relationship with the matrix. For very small precipitates, e.g., 1-5 unit

cells in the smallest dimension, interfacial energy is a predominant factor in determining the morphology. Generally, one habit will be at least slightly energetically more favorable than other possible habits and will predominate to the exclusion of the others. For similar thermodynamic reasons, it is unlikely that there is more than one orientation relationship with the matrix. Thus the observation of two habit planes ({210} and {110}) in a single microstructure wherein the precipitates are on the order of 2-3 unit cells in thickness suggests the presence of two distinct lath-like phases. Consideration has also been given to the possibility that the (110) precipitate is due to impurity effects, for example that ν is high enough that it is unlikely that trace impurities are responsible. Clearly, further work must be undertaken to determine whether a new phase is indeed present.

5. CONCLUSIONS

The Al-Cu-Li-Ag-Mg alloy Weldalite™ 049 exhibits a series of unusual and technologically useful combinations of mechanical properties in different aging conditions:

1. Natural aging without prior cold work to high strength (438 MPa YS, 585 MPA UTS),

2. A reversion temper of lower yield strength and unusually high ductility (25% elongation),

3. Room temperature re-aging of the reversion temper eventually leading to original T4 hardness, and

4. Ultra-high strength T6 properties (680 MPa YS, 720 MPA UTS).

Corresponding microstructures found to be responsible for these properties are:

1. Unusually well developed GP zone structure coupled with δ' in T4 temper,

2. Dissolution of δ' and coarsening (and some dissolution) of GP zones in reversion temper,

3. Reprecipitation of fine GP zones and δ' upon reversion plus natural aging,

4. A combination of several strengthening precipitates, including S', θ', and T_1 in the T6 temper.

In addition there is evidence of a fourth, previously unidentified precipitate, present as very thin laths on {110} planes, in the T6-type conditions. The persistence of these phases (plus the Zr-rich α') in the slightly overaged condition suggests the T6 condition may represent a metastable equilibrium between six phases.

6. ACKNOWLEDGEMENTS

Some of the data included in this section were obtained under sponsorship of the Martin Marietta Emerging Technology Fund and The National Institutes for Science and Technology (NIST).

7. REFERENCES

[1] J.R. Pickens, F.H. Heubaum, T.J. Langan, and L.S. Kramer, p.1397, Aluminum-Lithium Alloys (Proceedings of the Fifth International Aluminum-Lithium Conference, T.H. Sanders and E.A.Starke, eds., MCE Publications, Ltd, Birmingham, U.K., 1989).

[2] F.W. Gayle, J.R. Pickens, and F.H. Heubaum, ibid., p. 701.

[3] T.J. Langan and J.R. Pickens, ibid., p.691.

[4] I.J. Polmear and R.J. Chester, Scr. Metall. 23, 1213 (1989).

[5] A. Kelly and R. Nicholson, Progress in Materials Science, 10, 149 (1963).

[6] F.W. Gayle and J.B. VanderSande, Scr.Metall. 18, 473 (1984).

[7] P.J. Gregson and H.M. Flower, J.Mat.Sci.Letters 3, 829 (1984).

[8] A.M.Drits, N.A. Vorob'yev, A.M. Zinden, O.I. Voroshilova, Russ. Metall. 4, 142 (1981).

[9] R.K. Wyss and R.E. Sanders, Met.Trans.A 19A, 1988,pp.2523-2530.

[10] R. DeJesus and A.J. Ardell, Aluminum-Lithium Alloys, op.cit., p.661.

[11] A. Kelly and R. Nicholson, "Precipitation Hardening," Progress in Materials Science 10,pp. 149-392.

[12] R.N. Wilson and P.G. Partridge, Acta Metall. 13, 1321 (1965).

[13] V. Radmilovic, G. Thomas, G.J. Shiflet, and E.A. Starke, Scr. Metall. 23, 1141 (1989).

[14] A.K. Gupta, P. Gaunt, and M.C. Chaturvedi, Phil.Mag.A 55, 375 (1987).